Temperature dependence of Raman scattering in porous gallium phosphide

2001 J. Phys.: Condens. Matter 13 4579

(http://iopscience.iop.org/0953-8984/13/20/318)

INSTITUTE OF PHYSICS PUBLISHING JOURNAL OF PHYSICS: CONDENSED MATTER

J. Phys.: Condens. Matter **13** (2001) 4579–4589 www.iop.org/Journals/cm PII: S0953-8984(01)20203-3

Temperature dependence of Raman scattering in porous gallium phosphide

V V Ursaki[1], I M Tiginyanu[1], P C Ricci[2], A Anedda[2], E V Foca[3] and N N Syrbu[3]

[1] Laboratory of Low-Dimensional Semiconductor Structures, Institute of Applied Physics, Technical University of Moldova, 2004 Chisinau, Moldova
[2] INFM, Dipartimento di Fisica, Universitá di Cagliari, Cittadella Universitaria S P Monserrato-Sestu Km 0,700, 09042 Monserrato (Ca), Italy
[3] Centre of Nanoelectronics, Technical University of Moldova, 2004 Chisinau, Moldova

E-mail: ricci@alfis.dsf.unica.it

Received 18 December 2000, in final form 10 April 2001

Abstract

Porous layers fabricated by electrochemical anodization of (111)A-oriented n-GaP:Te substrates were studied by Raman scattering spectroscopy in the temperature interval from 10 to 300 K. Along with the transverse-optical (TO) and longitudinal-optical (LO) modes, the RS spectra of porous layers show Fröhlich-type vibrations located in the frequency gap between the bulk optical phonons. A longitudinal–transverse splitting of these surface-related vibrations was evidenced at low temperatures. Apart from that, the porous layers prepared on highly doped substrates were found to show LO-phonon–plasmon coupled (LOPC) modes in the whole temperature interval studied. Observation of LOPC modes at low temperatures is explained taking into account that the GaP skeleton consists of both depleted surface layers surrounding the pores and conductive regions. The free electrons in these regions, originating from the impurities actually located in the depletion layers, are shown to be subject to spatial confinement increasing with decreasing temperature.

1. Introduction

After the discovery of visible photoluminescence in porous Si by Canham [1], a great deal of interest has been paid to manufacturing and characterization of different porous materials including Si [2], Ge [3, 4], SiC [5, 6], III–V [7–14] and II–VI [15, 16] compounds. The experience gained shows that porosity represents an effective tool for engineering the band gap, band structure, phonon spectrum, refractive indices, resistivity, thermal conductivity etc of semiconductor materials. Spectacular changes in the material properties may occur at different characteristic dimensions l of the porous skeleton entities. When the dimensions involved are lower than the exciton Bohr radius, the quantum size effect on free carriers gives rise to a band gap increase and sharp modification of the optical and electrical properties. The exciton

Bohr radius a_b depends upon the nature of materials and is equal to ∼4.9 nm in Si, ∼14 nm in GaAs, ∼1.7 nm in GaP [2] etc. Considerable changes in specific material properties may occur, however, at characteristic dimensions l higher than the exciton Bohr radius provided that these dimensions correlate with or are much lower than the wavelength of the electromagnetic radiation. In the case of correlation, a strong diffuse scattering of light takes place in porous semiconductors leading to the onset of light localization [17, 18]. When the electromagnetic radiation with $\lambda \gg l$ propagates through porous structures of polar materials, the polarization of the skeleton entities in the electric field of radiation results in the excitation of electrical dipoles vibrating at specific frequencies located in the gap between the bulk optical phonons. These elementary excitations, predicted by Fröhlich [19], are called Fröhlich-type vibrations. In connection with strong tendencies to further miniaturization in modern electronics, one may expect the properties of many elements in optoelectronics circuits to be governed by Fröhlich vibrations. So, the study of Fröhlich vibrational modes becomes an important scientific task.

Fröhlich-type surface related vibrations were observed in porous structures of different III–V compounds [11, 14, 20–22]. In porous GaP, for instance, the Fröhlich mode frequency was found to depend upon the degree of porosity and dielectric function of the surrounding medium [14, 21–23]. Under hydrostatic pressure, an increase in the frequency gap between the Fröhlich mode and the LO phonon was observed and attributed to pressure-induced changes in the anharmonicity of the Fröhlich vibrations [24]. In this work, we present the results of a Raman scattering (RS) study of the first-order modes in porous GaP in the temperature interval from 10 to 300 K, with particular emphasis on Fröhlich vibrations and LO-phonon–plasmon coupling occurring in honeycomb-like porous GaP structures. A T–L splitting of the surface-related Fröhlich mode and regions with spatially confined free carriers were evidenced in the porous layers at low temperatures.

2. Experiment

(111)-oriented n-GaP substrates used in the present study were cut from Te-doped liquid-encapsulation-Czochralsky-grown ingots with the free electron concentrations $n_1 = 2 \times 10^{17}$ cm^{-3} and $n_2 = 1 \times 10^{18}$ cm^{-3} at 300 K. Porosity was introduced by anodic etching of samples for 30 min in a 0.5 M aqueous solution of sulphuric acid at the current density 5 mA cm^{-2} using a conventional electrochemical cell with a Pt working electrode. According to images obtained by a scanning electron microscope, the ∼10 μm thick porous layers possess a honeycomb-like morphology with quasi-uniformly distributed pores, the average pore and skeleton thickness being about 150 and 50 nm for samples with initial carrier concentrations n_1 and n_2 respectively (let us denote them as porous samples GaP-1 and GaP-2).

RS measurements on bulk GaP and porous specimens were carried out in a nearly backscattering geometry using a double spectrometer with spectral resolution less than 0.5 cm^{-1}. The samples mounted in an LTS-22-C-330 Workhorse-type optical cryogenic system were excited by the 488 nm line of an argon ion laser. To avoid local heating [14], the power of the laser beam was kept below 20 mW for a light spot diameter of about 100 μm on the sample surface.

3. Results and discussion

Figure 1 presents the RS spectra of porous samples GaP-1 and GaP-2 at different temperatures. Like bulk GaP, the porous samples show at 300 K an intense TO peak at ∼365 cm^{-1} with a pronounced asymmetric shape. With decreasing temperature, a narrowing of the peak occurs,

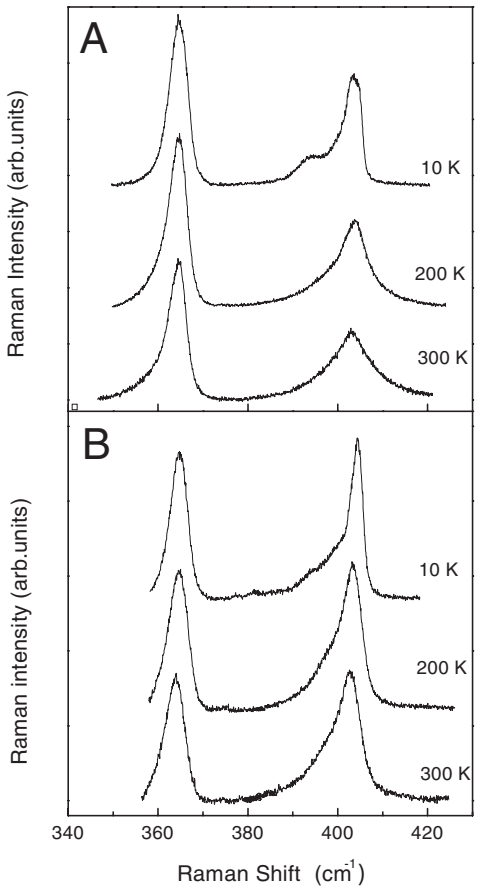

Figure 1. Raman spectra from porous samples at different temperatures: (A) GaP-1, (B) GaP-2.

accompanied by a decrease of the band asymmetry in the low-energy wing. According to [25], the asymmetric TO band shape under ambient conditions is caused by the third-order anharmonic interaction of the $\boldsymbol{q} \sim \mathbf{0}$ TO phonons with the nearly degenerate sum combination (358 cm^{-1}) of the TA(X) and LA(X) vibrations. The changes in the TO band shape with decreasing temperature may be attributed to a weakening of the anharmonic interaction involved.

As to the RS spectra in the vicinity of the bulk LO mode, they exhibit a complex structure (figure 1). Figure 2 illustrates the RS spectra of both bulk and porous GaP samples in the region of the zone-centre LO phonon ($\sim$403 cm^{-1}) measured at 300 K. The low doped substrate shows a pure LO phonon while the high doped substrate exhibits a LO band possessing a well pronounced shoulder on the high-energy wing. As one can see from figure 2, porosity induces considerable changes in the RS spectra of both low and high doped GaP. According to the results of a spectral decomposition (figure 3), along with the LO-phonon peak, both porous samples GaP-1 and GaP-2 show a broad RS band marked 'F' with the maximum at $\sim$400 cm^{-1}. A similar band was observed in porous GaP earlier and attributed to a Fröhlich vibrational mode [14]. The origin of the large width of this band will be discussed below.

Apart from the LO and Fröhlich bands, the porous sample GaP-2 shows a relatively broad peak with the maximum at $\sim$408 cm^{-1}. Such a peak is inherent also to bulk highly doped GaP (figure 3(c)). Taking into account the upward frequency shift of this band in comparison

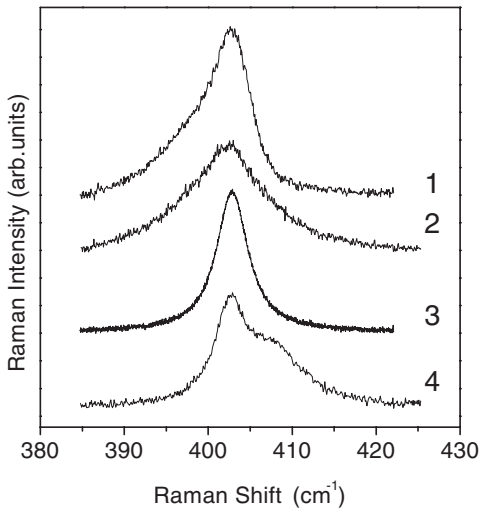

Figure 2. Raman spectra from the bulk and from porous GaP samples in the region of the LO mode at room temperature: (1) porous sample GaP-1; (2) porous sample GaP-2; (3) bulk sample GaP-1; (4) bulk sample GaP-2.

with the position of the pure LO phonon, one may consider the interaction between lattice vibrations and free carrier plasma as a possible reason for its occurrence.

It is well known [26] that in doped polar semiconductors the plasmon interacts with the LO phonon and the RS spectra are dominated by the LO-phonon–plasmon coupled modes (LOPC), usually denoted by L_- and L_+, instead of the LO phonon. The features of this interaction was studied systematically in GaAs and other III–V compounds [20, 26–28]. It was found, in particular, that in contrast to the case of GaAs [28] the L_- mode cannot be observed in GaP due to strong damping caused by the low mobility of free carriers [26]. On the other hand, the simultaneous observation of the LO-phonon–plasmon mode L_+ and of the 'unscreened' LO phonon (figures 3(b),(c)) hints at the existence of regions with quite different concentrations of free carriers in both bulk and porous GaP-2 samples.

With decreasing temperature, the Raman scattering intensity was found to increase monotonically. At 10 K, along with the pure LO phonon, the porous sample GaP-1 exhibits two low-frequency modes marked 'F1' and 'F2' with the maxima at 394.5 and 401 cm^{-1}, respectively (figure 4(a)). Similar peaks were evidenced by the spectral decomposition performed in the porous GaP-2 sample as well (figure 4(b)). Apart from that, as in the case of RS measurements at room temperature (figure 3(b)), this sample shows a RS peak at a frequency higher than the frequency of the pure LO band (figure 4(b)). Unlike the porous sample GaP-2, the substrate shows at 10 K only one RS peak at 404 cm^{-1} corresponding to the pure LO phonon. Below we will analyse the reasons giving rise to the observed difference in the temperature dependence of RS in bulk and porous GaP-2.

III–V compounds, and GaP in particular, are characterized by the existence of a surface depleted layer with the thickness

$$L_D = (2\varphi_0\varepsilon_0\varepsilon_S/eN_D^+)^{1/2} \tag{1}$$

where $e\varphi_0 = 0.8$ eV is the surface potential, $\varepsilon_0\varepsilon_S$ is the static dielectric constant of the material and N_D^+ is the concentration of ionized donors. For the given concentrations of free carriers, at room temperature the L_D is equal to ∼50 and ∼20 nm respectively for bulk samples GaP-1

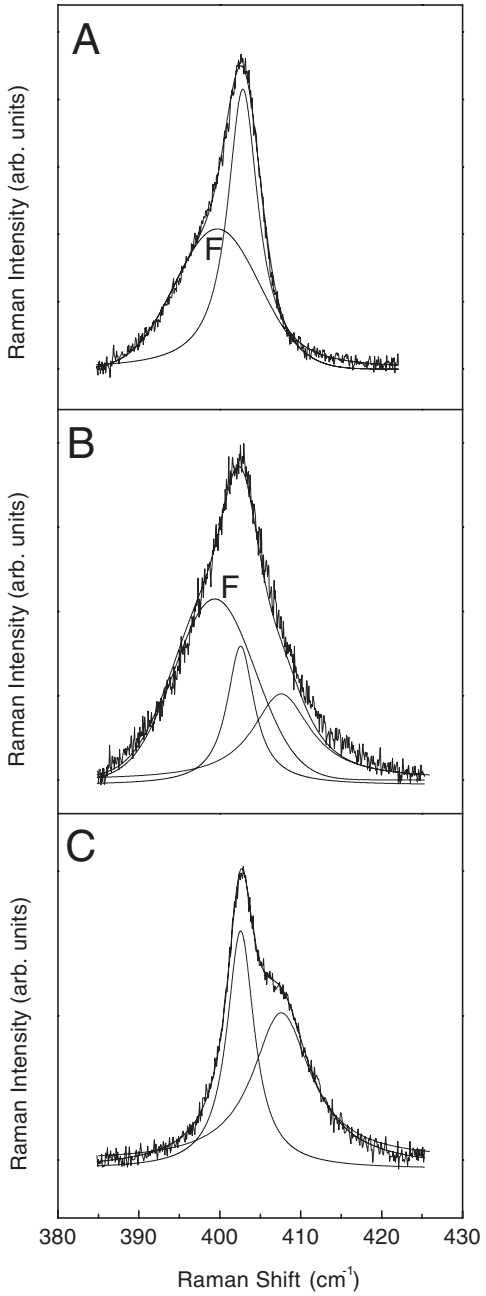

Figure 3. Decomposition of the Raman spectra in the region of LO-phonon scattering at room temperature, from (A) porous sample GaP-1; (B) porous sample GaP-2; (C) bulk sample GaP-2.

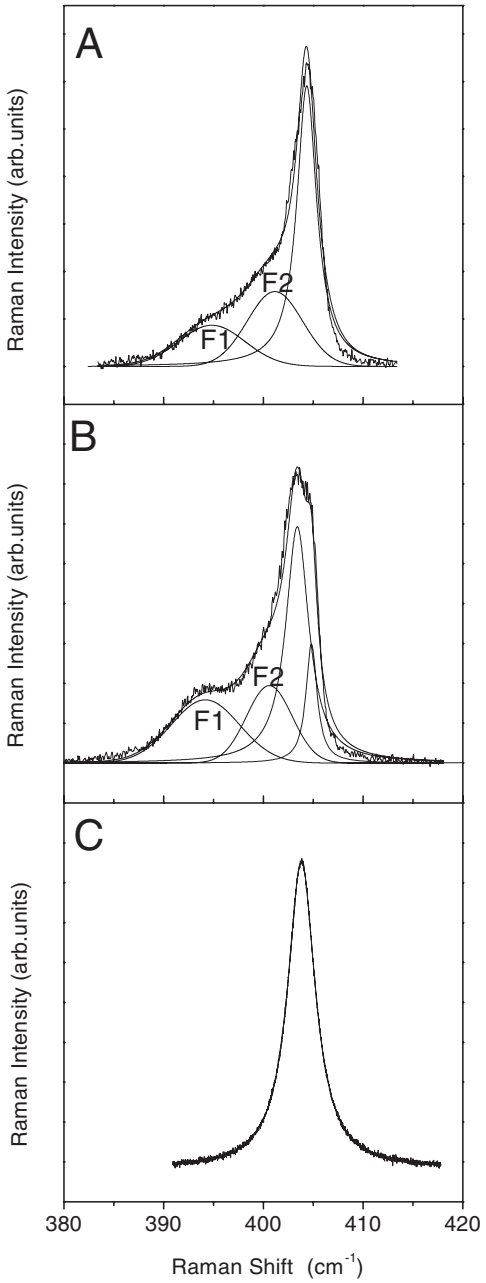

Figure 4. Decomposition of the Raman spectra in the region of LO-phonon scattering at 10 K, from (A) porous sample GaP-1; (B) porous sample GaP-2; (C) bulk sample GaP-2.

and GaP-2. Taking into account the wavelength of the exciting light (488 nm) and the band gap of GaP ($E_g = 2.24$ eV at 300 K) [29], it is obvious that the laser beam provides the excitation of a layer with the thickness of about a few hundred nanometres. Under such conditions of

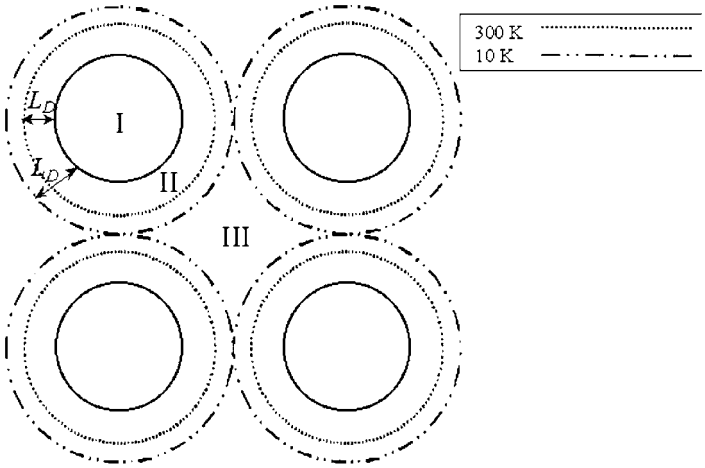

Figure 5. Representation of the volume distribution within a porous membrane: (I) pore volume; (II) depleted GaP volume; (III) GaP volume containing free charge carriers. The dotted line shows the depletion layer at room temperature, the dash–dot line that at 10 K.

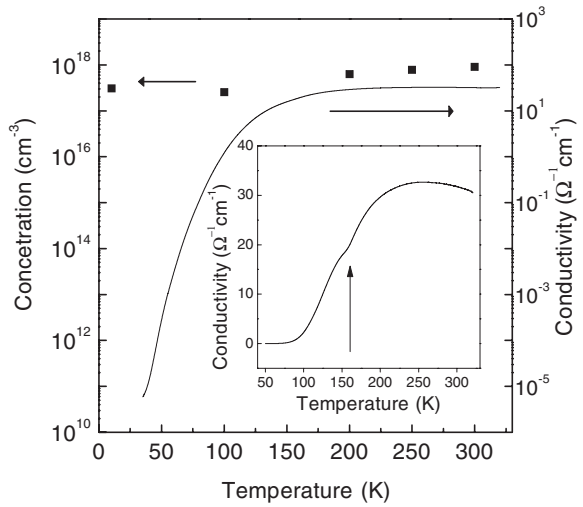

Figure 6. The curve shows the dark conductivity at different temperatures, the symbols the concentration of free carrier as determined by Raman scattering in the highly doped GaP sample (GaP-2). The inset represents the thermally stimulated conductivity.

excitation one may expect both surface depleted layers and bulk areas containing free carriers to contribute to the Raman scattering. Indeed, as one can see from figure 3(c), the RS spectra of highly doped GaP substrate shows both the LO and LOPC modes. The 'unscreened' LO phonon comes from the surface depleted layer, while the L_+ mode originates from the deeper regions where the coupling between LO phonon and plasmon dominates. Unlike bulk GaP-2, the substrate GaP-1 shows only the LO peak in the RS spectrum (figure 2), thus reflecting the absence of plasmon excitations at the electron concentration n_1.

With decreasing temperature, the concentration of free carriers should diminish due to their trapping. One may expect, therefore, at sufficiently low temperatures the RS spectra of highly doped GaP to be dominated by the pure LO phonon. Indeed, as seen from figure 4(c), at 10 K

the highly doped substrate shows only a peak corresponding to the unscreened LO phonon. At the same time the porous sample GaP-2 exhibits an L_+ mode in the whole temperature interval studied, including 10 K (see figure 4(b)). This result demonstrates the existence of high density of free carriers in the porous layer even at 10 K.

As shown recently [23], the free carrier distribution in porous GaP structures at room temperature is highly inhomogeneous. Depending upon the value of L_D, a part of the porous skeleton contains no free carriers. It consists of carrier exhausted areas surrounding the pores. Another part, covering the remaining regions of the GaP skeleton, contains free carriers and contributes to the occurrence of L_+ modes. Comparing the value of L_D ($\approx$20 nm) with the thickness of the walls ($\approx$50 nm) between pores in sample GaP-2, the spatial distribution of pores 'I', exhausted areas 'II' and regions 'III' containing free carriers can be represented as shown in figure 5. Note that at room temperature the exhausted areas do not touch each other thus leaving space for free carriers to move freely along the honeycomb-like structure. With decreasing temperature, however, free carrier trapping in the region 'III' takes place. On the one hand, it leads to the increase in L_D and, in consequence of this, to the expansion of the exhausted areas up to overlapping, as illustrated in figure 5. On the other hand, not all free carriers confined in the region 'III' can be trapped. Indeed, assuming that the ionized donors are uniformly distributed along the GaP skeleton, it is obvious that only some of them are placed in the region 'III' and can participate in the free carrier trapping with decreasing temperature. The ionized donors from the region 'II' cannot contribute to the charge carrier trapping and, therefore, the free electrons originating from these donors remain in the conduction band down to very low temperatures.

It is interesting to note that, in case of overlapping of the exhausted areas, the free carriers will be confined in column-like structures. One may expect, therefore, a sharp reduction with decreasing temperature in the porous structure conductivity measured in the direction perpendicular to pores. To verify this, ohmic contacts were prepared by vacuum evaporation of Ni–AuGe–Ni with subsequent rapid thermal annealing [30] on the top surface of a porous layer of GaP-2 detached from the substrate. As expected, the dark conductivity of this layer shows a decrease of more than six orders of magnitude with lowering the temperature from about 160 to 10 K (figure 6).

Figure 6 illustrates also the thermally stimulated conductivity spectrum taken from the GaP-2 porous sample after white light (tungsten lamp) illumination for 30 seconds at 10 K with a thermal scan at a rate of 0.1 K s^{-1}. In our opinion the photo-excited carriers are as well confined in the regions 'III' at low temperatures. The feature marked in the TSC curve by an arrow is indicative of the release of the confined carriers from the regions 'III' at about 160 K. At this temperature the exhausted areas no longer overlap due to the increase of conductivity and decrease of L_D. Under such conditions the photo-excited carriers can move freely along the honeycomb-like structure.

To calculate the free electron concentration in the regions 'III', the L_+ mode in the RS spectra of porous sample GaP-2 was analysed as a function of temperature. The analysis was based on the computer simulation of the RS spectra in the vicinity of the LO frequency taking into account the LO mode of the Lorentzian form, two L and T surface modes of Gaussian form and a band caused by the LO-phonon–plasmon coupling.

Raman scattering from LO-phonon–plasmon-coupled modes is defined by the following mechanisms:

(A) modulation of the optical polarizability by the atomic displacement (deformation potential scattering) and by the macroscopic longitudinal electric field (electrooptical scattering),

(B) scattering due to density fluctuations of the free carriers.

According to [31], Raman efficiencies due to the mechanisms (A) and (B) can be converted as proportional to

$$S_A(\omega) = [(\omega_0^2 - \omega^2)/(\omega_T^2 - \omega^2)]^2 x \text{ Im } -\{1/[\varepsilon(q,\omega)]\} \tag{2}$$

and

$$S_B(\omega) = [(\omega_L^2 - \omega^2)/(\omega_T^2 - \omega^2)]^2 x \text{ Im } -\{1/[\varepsilon(q,\omega)]\} \tag{3}$$

where $\omega_0^2 = \omega_T^2(1 + C)$, C being the Faust–Henry coefficient [32], and ω_T and ω_L are the TO and LO mode frequency, respectively.

$\varepsilon(q,\omega)$ is the total dielectric function of the LOPC system and takes the familiar Drude form

$$\varepsilon(q,\varpi) = \varepsilon_\infty \left[1 + \frac{\varpi_L^2 - \varpi_T^2}{\varpi_T^2 - \varpi^2 - \mathrm{i}\gamma\varpi} - \frac{\varpi_P^2(q)}{\varpi^2 - \mathrm{i}\Gamma_P\varpi}\right]. \tag{4}$$

In this expression ε_∞ is the high-frequency dielectric constant; γ and Γ_P are the phenomenological damping constants of the atomic and free-carrier oscillations, respectively. $\omega_P(q)$ is the plasma frequency given as a function of the carrier density N by the relation

$$\omega_P^2(q) = (4\pi N e^2)/(\varepsilon_\infty m^*) + 3/5(qV_F) \tag{5}$$

where m^* is the free-carrier effective mass and V_F is the Fermi velocity

$$V_F = (\hbar/m^*)(3\pi^2 N)^{1/3}. \tag{6}$$

For a quasi-backscattering geometry one can take the scattering wave vector as $|\boldsymbol{q}| = 4\pi n/\lambda_L$, where n is the refractive index of GaP at the laser wavelength $\lambda_L = 488$ nm.

In cases of large effective carrier masses the light scattering efficiency S_A via deformation potential and electrooptic mechanisms dominates, and the contribution S_B due to charge density fluctuations is negligible [33]. As to the effective mass m^*, the bare mass rather than the (experimentally measured) polaron mass has to be used [34]. According to Beni and Rice [35], the values of the bare masses for electrons in GaP are $m_\parallel = 1.781\ m_0$, $m_\perp = 0.25\ m_0$. The effective mass then is given by

$$m^* = \left[\frac{1}{3}\left(\frac{2}{m_\perp} + \frac{1}{m_\parallel}\right)\right]^{-1} = 0.35 m_0. \tag{7}$$

Using relations (4)–(6) in the limit of negligible phonon damping one can write for S_A

$$S_A = [\omega_P^2 \omega \Gamma_P(\omega_0^2 - \omega^2)]/\Delta \tag{8}$$

where

$$\Delta = [\omega^2(\omega_L^2 - \omega^2) - \omega_P^2(\omega_T^2 - \omega^2)]^2 + \omega^2\Gamma_P^2(\omega_L^2 - \omega^2)^2. \tag{9}$$

Assuming that the average scattering time τ of the carriers is equal to $(\Gamma_P)^{-1}$, a simple relationship between carrier mobility and damping constant is obtained:

$$\mu = |e|/(m^*\Gamma_P). \tag{10}$$

For high mobility values when $\Gamma_P \ll \omega_P$, the peaks of S_A are mainly determined by the zeros of the first term of the denominator leading to the well known LOPC frequencies:

$$\omega_\pm^2 = [(\omega_L^2 + \omega_P^2)/2] \pm \{[(\omega_L^2 + \omega_P^2)/2]^2 - \omega_P^2\omega_T^2\}^{1/2} \tag{11}$$

and the RS spectrum consists of two peaks located at the frequencies ω_- and ω_+.

For low values of mobility, when $\Gamma_P \sim \omega_P$, one of the ω_- or ω_+ signals decreases rapidly below the detection limit, while the remaining one is strongly broadened and shifts towards

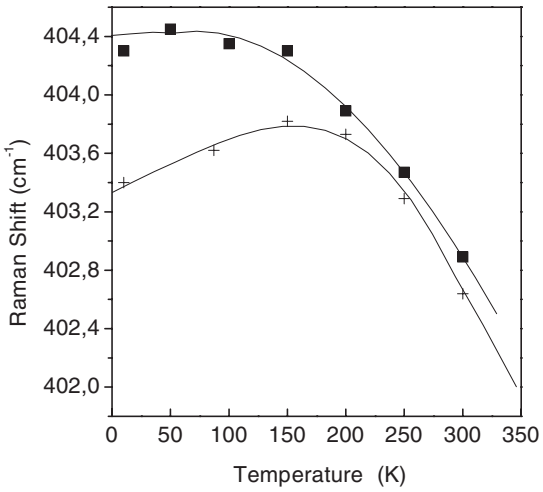

Figure 7. Raman shift of the LO mode with temperature: ■, porous sample GaP-1; +, porous sample GaP-2 [1].

the LO or TO frequency with decreasing mobility. In our experiments the ω_- intensity is vanishing and the LOPC signal is determined by the ω_+ peak.

Analytical adjustment using a standard fitting procedure allowed us to determine the main electrical parameters of the samples: carrier concentration and mobility. The derived data on free electron concentration at different temperatures are summarized in figure 6. One can see that the concentration of charge carriers decreases insignificantly with the temperature decrease from 300 to 10 K.

Another effect of the carrier confinement is the unusual dependence of the LO-mode shift with temperature. As illustrated in figure 7, starting from the temperature of about 160 K, a downward frequency shift of the LO mode occurs in the GaP-2 porous sample with decreasing temperature. This mode softening can be explained taking into account the existence of strong electric fields between exhausted areas 'II' and regions 'III' with high free carrier concentration. Evidently, the built-in electric fields achieve especially high values when the free carriers start to be confined in column-like structures.

Strain induced by free carriers is a common feature of confined systems. It was shown that carrier induced strain may explain many of the unusual properties of porous silicon [36]. A carrier-induced strain model was proposed to explain the optical properties of Si and GaAs nanocrystals [37].

The average stresses in material can be estimated from the shifts of the LO phonon [38]. Investigation of porous GaP under hydrostatic pressure [24] showed that elastic properties of porous GaP do not differ essentially from those of bulk material. The frequency of the LO mode in bulk and porous GaP increases linearly with pressure at the rate of 0.4 cm^{-1} $kbar^{-1}$. One can deduce from the results of these investigations that the shift of the LO mode of 1 cm^{-1} corresponds to the pressure of $\sim$2.5 kbar. Taking into account the decrease of the LO frequency in our structures at temperatures below 160 K one can conclude that the strains are tensile rather than compressive. Additional investigations are necessary to evaluate the built-in electric fields, since the piezoelectric constants of the material depend upon the orientation, temperature, carrier concentration etc. One can perform a rough estimation of these values. Anastassakis calculated the electric fields of $\sim 7 \times 10^6$ V m^{-1} [39] in GaAs for the appropriate values of strains. Taking into consideration the appropriate values of elastic constants of GaP

and GaAs [40], one can estimate the built-in electric fields in our samples at $T < 160$ K to be of the same order. On the other hand, calculation of the electric fields between the exhausted regions and regions with the carrier concentration of 10^{18} cm^{-3} and the dimensions of ∼50 nm gives values of $\sim 5 \times 10^6$ V m^{-1}.

So, in spite of the sharp reduction of in-plane conductivity, the porous layer GaP-2 contains regions with a relatively high concentration of free carriers even at temperatures as low as 10 K. A comparative analysis of the obtained results shows that the free electrons are confined in column-like areas. As a result, the layer conductivity is highly anisotropic, its minimum value being observed in the directions perpendicular to the pores.

The observation of two RS peaks F1 and F2 at low temperatures (figure 4) may be attributed to the longitudinal–transverse (L–T) splitting of the Fröhlich mode [22]. One can note that the L–T splitting of a Fröhlich mode was observed recently [41, 42] in porous structures of SiC, GaP and InP compounds by Fourier transform infrared spectroscopy. Theoretical considerations of the observed splitting were carried out [41, 42] in terms of effective medium expressions for the dielectric function. Note that in the case of infrared reflectance investigations the wavelength of electromagnetic radiation proves to be much larger than the lateral dimensions of pores and pore walls and, therefore, the porous structure can be considered as a homogeneous material for which the effective medium approaches apply.

4. Conclusion

First order Raman spectra of porous GaP layers contain Fröhlich-type vibrations in addition to the TO and LO modes inherent to bulk material. The longitudinal–transverse splitting of the Fröhlich mode in Raman spectra was observed for the first time in a porous III–V compound at low temperatures. Both bulk and porous GaP possessing free electrons with the concentration as high as $n \sim 10^{18}$ cm^{-3} show LO-phonon–plasmon coupling at room temperature. In contrast to bulk material, porous GaP layers exhibit LOPC modes also at low temperatures. The analysis of Raman scattering from the LOPC modes along with the data of electrical characterization and thermally stimulated conductivity indicate the formation of high conductivity ($n \sim 10^{18}$ cm^{-3}) regions with the dimensions of ∼50 nm embedded in a low conductivity porous GaP matrix at temperatures lower than 160 K. The spatial confinement of free electrons in these regions leads to the appearance in porous GaP structures of strong built-in electric fields estimated at 5×10^6 V m^{-1}.

Acknowledgment

The authors would like to thank Professor J Monecke for fruitful discussions.

References

[1] Canham L T 1990 *Appl. Phys. Lett.* **57** 1046
[2] Cullis A G, Canham L T and Calcott P D J 1997 *J. Appl. Phys.* **82** 909
[3] Miyazawa S, Sakamoto K, Shiba K and Hirose M 1995 *Thin Solid Films* **255** 99
[4] Sendova-Vassileva M, Tzenov N, Dimova-Malinovska D, Rosenbauer M, Stutzman M and Josepovits K V 1995 *Thin Solid Films* **255** 282
[5] Shor J S, Grimberg I, Weiss B Z and Kurtz A D 1993 *Appl. Phys. Lett.* **62** 2836
[6] Takazawa A, Tamura T and Yamada M 1993 *Japan. J. Appl. Phys.* I **32** 3148
[7] Takizawa T, Arai S and Nakahara M 1994 *Japan. J. Appl. Phys.* I **33** 643
[8] Ludwig M H, Hummel R E and Chang S S 1994 *J. Vac. Sci. Technol.* B **12** 3023
[9] Belogorokhov A I, Karavanskii V A, Obraztsov A N and Timoshenko V Yu 1994 *JETP Lett.* **60** 275

[10] Erne B H, Vanmaekelbergh D and Kelly J J 1995 *Adv. Mater.* **8** 739
[11] Anedda A, Serpi A, Karavanskii V A, Tiginyanu I M and Ichizli V M 1995 *Appl. Phys. Lett.* **67** 3316
[12] Schmuki P, Fraser J, Vitus C M, Graham M S and Isaacs H S 1996 *J. Electrochem. Soc.* **143** 3316
[13] Schmuki P, Lockwood D J, Labbe H J and Fraser J W 1996 *Appl. Phys. Lett.* **69** 1620
[14] Tiginyanu I M, Irmer G, Monecke J and Hartnagel H L 1997 *Phys. Rev.* B **55** 6739
[15] Hoyer P, Baba N and Masuda H 1995 *Appl. Phys. Lett.* **66** 2700
[16] Zenia F, Levy-Clement C and Triboulet R 1999 *Appl. Phys. Lett.* **75** 531
[17] Schuurmans F J P, Vanmaekelbergh D, van de Lagemaat J and Lagendijk A 1999 *Science* **284** 141
[18] Schuurmans F J P, Megens M, Vanmaekelbergh D and Lagendijk A 1999 *Phys. Rev. Lett.* **83** 2183
[19] Fröhlich H 1949 *Theory of Dielectrics* (Oxford: Clarendon)
[20] Tiginyanu I M, Irmer G, Monecke J, Vogt A and Hartnagel H L 1997 *Semicond. Sci. Technol.* **12** 491
[21] Kuriyama K, Ushiyama K, Ohbora K, Miyamoto Y and Takeda S 1998 *Phys. Rev.* B **58** 1103
[22] Tiginyanu I M and Hartnagel H L 1999 *GaAs'99 Conf. Proc. (Munich, 1999)* (Miller Freeman) pp 194–9
[23] Sarua A, Tiginyanu I M, Ursaki V V, Irmer G, Monecke J and Hartnagel H L 1999 *Solid State Commun.* **112** 581
[24] Tiginyanu I M, Ursaki V V, Raptis Y S, Stergiou V, Anastassakis E, Hartnagel H L, Vogt A, Prevot B and Schwab C 1999 *Phys. Status Solidi* b **211** 281
[25] Barker A S Jr 1968 *Phys. Rev.* **165** 197
[26] Abstreiter G, Cardona M and Pinczuk A 1975 *Light Scattering in Solids* ed M Cardona (Berlin: Springer) p 147
[27] Gargouri M, Prevot B and Schwab C 1987 *J. Appl. Phys.* **62** 3902
[28] Prevot B and Wagner J 1991 *Prog. Cryst. Growth Charact.* **22** 245
[29] Aspnes D E and Studna A A 1983 *Phys. Rev.* B **27** 985
[30] Miao J, Tiginyanu I M, Hartnagel H L, Irmer G, Monecke J and Weiss B L 1997 *Appl. Phys. Lett.* **70** 847
[31] Klein M V, Ganguly B N and Colwell P J 1972 *Phys. Rev.* B **6** 2380
[32] Faust W L and Henry C R 1966 *Phys. Rev. Lett.* **17** 1265
[33] Irmer G, Wenzel M and Monecke J 1997 *Phys. Rev.* B **56** 9524
[34] Irmer G, Toporov V V, Bairamov B H and Monecke J 1983 *Phys. Status Solidi* b **119** 595
[35] Beni G and Rice T M 1978 *Phys. Rev.* B **18** 768
[36] Zhao Xue-Shu, Persans P D and Schroeder J 1995 *High Pressure Science and Technology. Proc. Joint 15th AIRAPT 33rd EHPRG Int. Conf.* ed W A Trzeciakowski (Warsaw) p 600
[37] Zhao Xue-Shu, Schroeder J and Persans P D 1994 *Appl. Phys. Lett.* **65** 2033
[38] Cerdeira F, Buchenauer C J, Pollak F H and Cardona M 1972 *Phys. Rev.* B **5** 580
[39] Anastassakis E 1992 *Phys. Rev.* B **46** 4744
[40] Simmons G and Wang H 1971 *Single Crystal Elastic Constants and Calculated Aggregate Properties* (Cambridge, MA: MIT Press) p 28
[41] MacMillan M F, Devaty R P, Choyke W J, Goldstein D R, Spanier J E and Kurtz A D 1996 *J. Appl. Phys.* **80** 2412
[42] Sarua A, Gärtner G, Irmer G, Monecke J, Tiginyanu I M and Hartnagel H L 2000 *Phys. Status Solidi* a **182** 207